INFRARED VERSUS LIGHT SCATTERING TECHNIQUES TO MONITOR THE GEL TO LIQUID CRYSTAL PHASE TRANSITION IN LIPID MEMBRANES

short title: **Lipid membrane phase transition: IR vs. light scattering**

Paola Sassi[1,*], Silvia Caponi[2], Maria Ricci[1], Assunta Morresi[1], Harriëtte Oldenhof[3], Willem F. Wolkers[4] and Daniele Fioretto[5,6]

[1] Department of Chemistry Biology and Biotechnologies, University of Perugia, Italy

[2] Istituto Officina dei Materiali del CNR (CNR-IOM) - Unità di Perugia, c/o Dipartimento di Fisica e Geologia, Perugia, Italy

[3] Clinic for Horses - Unit for Reproductive Medicine, University of Veterinary Medicine Hannover, Germany

[4] Institute of Multiphase Processes, Leibniz Universität Hannover, Germany

[5] Dipartimento di Fisica e Geologia, Università di Perugia, Italy

[6] Centro di Eccellenza sui Materiali Innovativi Nanostrutturati (CEMIN), Università di Perugia, Italy.

[*]**correspondence to:** Paola Sassi, Department of Chemistry, Biology and Biotechnology, University of Perugia, Perugia, Italy. phone: +39 075 5855585; fax: +39 075 5855586; e-mail: paola.sassi@unipg.it

keywords: FTIR spectroscopy, Infrared spectroscopy, Raman spectroscopy, Brillouin spectroscopy, lipid phase behavior

ABSTRACT

In this study, Fourier transform infrared, Raman as well as Brillouin spectroscopy have been used to study lipid phase behavior of hydrated as well as dried multilamellar L-α-phosphatidylcholine assemblies, in order to compare limitations and potentials of the different techniques. Dried lipid samples have been studied in the presence and absence of trehalose, which is known to affect the phase behavior of these systems. The methylene C-H stretching (2800-3000 cm^{-1}) region in IR and Raman spectra provided mutually consistent information on the rearrangement of lipid acyl chains occurring at the lipid melting temperature. IR spectra have a higher signal to noise ratio, thus permitting a more precise evaluation of the melting temperature. In the hydrated lipid samples, the CH stretching region in the Raman spectra is less affected by the contribution of water compared to that in the IR spectra. Raman spectra are particularly suitable to simultaneously study both lipid and water contributions allowing to distinguish ice from non-frozen water below 0 °C. Brillouin light scattering was used to probe the collective dynamics, i.e. the propagation velocity and the attenuation of longitudinal acoustic modes in the lipid samples. Lipid phase transitions are evident from a change in the temperature behavior of the acoustic velocity. Moreover, a strong relaxation process with a characteristic time of 14 ps was observed in the sample dried without trehalose with a maximum in acoustic attenuation at about 45°C, which likely reflects the rearrangement of acyl chains.

INTRODUCTION

Cell membranes are composed of a complex mixture of phospholipids, cholesterol and proteins. Phosphatidylcholine (PC) is the most abundant phospholipid in cell membranes. Liposomes composed of one type of lipid or mixtures of lipids have been used to study properties of biological membranes. Lamellar lipid assemblies undergo radical changes in physical state over narrow temperature ranges at a characteristic phase transition temperature [1]. Lipid phase transitions occur at specific temperatures for each lipid depending on head group type, chain length, chain saturation, hydration, and thermal history. The bilayer below the main phase transition temperature exists in a closely packed gel state, with the acyl chains relatively immobilized in a tightly packed array. In the more fluid, liquid crystalline state, there is relatively more conformational disorder [2]. Not only, temperature, but also the hydration state of the lipid head groups, determines the lipid phase state. Dehydration may cause membranes to undergo fluid to gel phase transitions [3-5].

Many techniques are available to study lipid phase behavior, including differential scanning calorimetry (DSC), Raman and infrared spectroscopy, X-ray diffraction (XRD), NMR, fluorescence spectroscopy, and computer simulations. One major drawback of high sensitivity methods such as fluorescence and electron spin resonance (ESR) is that there is a need for labeling and that the influence of the probe on the structure and behavior of the system must be considered. Vibrational spectroscopic methods such as Raman and infrared spectroscopy do not require labeling and can be used to accommodate aqueous as well as dry samples with minimal sample preparation. Fourier transform infrared (FTIR) is widely used to monitor lipid phase behavior during changes in temperature or during drying [5-7]. Lipid phase behavior can be studied by monitoring the temperature dependence of the symmetric or antisymmetric CH_2 stretching bands at 2850 cm^{-1} and 2920cm^{-1}, respectively [8]. Raman

spectroscopy is not as widely used as FTIR to study lipid phase behavior, which is likely due to the generally higher signal to noise ratio of infrared spectra compared to that of Raman spectra. Raman spectroscopy is also based on measurements of molecular vibrations. Changes in lipid membrane structure can be observed by monitoring relative Raman peak intensities that represent intra-and intermolecular order, which, in turn, are indicators of lipid phase changes. The methylene C-C stretching (1030-1150 cm^{-1}) and the methylene C-H stretching (2800-3100 cm^{-1}) regions are used as indicators of membrane order [9,10], but phase changes can also be detected by observing peak shifts [11,12]. With a confocal-Raman microscope, it is possible to optically trap individual liposomes so that Raman scattering is collected from one liposome while minimizing contributions from the surrounding solution [13]. Just like Raman scattering, Brillouin light scattering (BLS) describes the inelastic scattering of light from vibrations of matter. However, while in Raman spectroscopy photons are scattered by interaction with vibrational and rotational transitions in molecules, Brillouin spectroscopy involves the scattering of photons from low-frequency (GHz) collective acoustic modes, the acoustic phonons. BLS has been used for measuring the viscoelastic behavior of a large variety of samples ranging from liquids [14] to polymeric [15] and biological systems [16]. The elastic characterization of oriented lipid multibilayers has been obtained by angle resolved BLS measurements [17,18]. The collective short wavelength dynamics of lipid membranes has also been studied using inelastic neutron scattering. The corresponding dispersion relation for the gel and the liquid phases of lipid bilayers provides information on the phase transition and the respective phase coexistence [19].

In this study, FTIR, Raman and Brillouin spectroscopy are used to study the lipid phase behavior of hydrated and dried multilamellar L-α-phosphatidylcholine assemblies and its influence on localized and collective dynamics. The C-H stretching (2800-3000 cm^{-1}) regions in IR and Raman spectra are analyzed to monitor the change in packing of the acyl

chains occurring at the phase transition, and to identify similarities and differences between the two spectroscopic techniques. Brillouin spectroscopy was used to measure the propagation velocity and attenuation of longitudinal acoustic modes, giving information on the evolution of the elastic properties coinciding with the phase change and the relaxation of density fluctuation.

MATERIALS AND METHODS

Preparation of liposomes

L-α-phosphatidylcholine (Egg, Chicken) dissolved in chloroform was purchased from Avanti Polar Lipids. The chloroform of the 25 mg ml^{-1} lipid solution was allowed to evaporate in a fume hood. The solution was then placed in a desiccator where pressure was reduced by a vacuum pump for at least 12 hours. The end result of this evaporation was a lipid film cake. Hydration of this lipid film was accomplished by adding water to achieve a lipid concentration of 40 mg ml^{-1}. The solution was then agitated, and the hydrated lipid suspension underwent 3 freeze/thaw cycles by alternately placing the sample vial in liquid nitrogen and in warm water. This procedure yields stacked multilamellar vesicles.

Fourier transform infrared spectroscopy (FTIR)

Infrared absorption measurements were carried out with a Perkin-Elmer 100 Fourier transform infrared (FTIR) spectrometer (Perkin Elmer, Norwalk, CT, USA), equipped with a narrow band Mercury/Cadmium/Telluride liquid nitrogen cooled IR-detector. The optical

bench was continuously purged with dry air from an FTIR purge gas generator (Whatman, Clifton, NJ, USA). The acquisition parameters were: 4 cm^{-1} resolution, 8 co-added interferograms, 4000-900 cm^{-1} wavenumber range. Spectra analysis and display were carried out using Perkin-Elmer software (Perkin-Elmer, Norwalk, CT, USA).

For FTIR analysis 10 μL of lipid solution was sandwiched between two CaF2 windows. Dried samples were prepared by drying 10 μL of lipid solution on a CaF2 window for 3 h under a flow of dry air (less than 3% RH). Drying in the presence of trehalose was done using lipid/trehalose mass ratios of 1/2. Dried samples were heated up to 80 °C for 10 min prior to FTIR analysis samples to remove residual water.

A variable temperature FTIR sample holder with heater device (Harrick Scientific Products, Pleasantville, NY, USA) together with a Linkam pump system using liquid nitrogen as a coolant (Linkam Scientific Instruments, Tadworth, Surrey, UK) were used for temperature-dependent FTIR measurements. The sample temperature was monitored using a thermocouple that was located close to the sample.

The temperature dependence of the FTIR spectra was studied by cooling the sample from 20 °C to temperatures as low as -50 °C at a rate of approximately 1 °C min^{-1}. The sample was subsequently heated with 1 °C/min, while acquiring FTIR spectra every 30 s. Membrane fluidity was monitored by observing the position of the CH_2 symmetric stretching band at approximately 2850 cm^{-1}, as previously described [8]. Briefly, second derivatives of the IR spectra were taken using a thirteen-point smoothing factor, the 2865 to 2835 cm^{-1} region was selected and normalized, and the position of the symmetric CH_2 stretching vibration absorbance band (νCH_2) was calculated by taking the average of the spectral positions at 80% of the band height. The νCH_2 lipid band position was plotted versus the sample temperature, and phase transition temperatures were determined from the maxima in

the first derivatives of the νCH_2 versus temperature plots. Averages ± standard deviations were calculated from 2-4 measurements.

Raman Spectroscopy

Raman spectra were obtained using a micro-Raman setup equipped with a λ=514.5 nm excitation of an Argon Ion laser (Coherent mod. Innova 90) at ca. 20 mW power. A back scattering geometry was realized using the 50x long working distance objective of an OLYMPUS microscope MOD BX40. The scattered radiation was analyzed by a single monochromator Horiba Jobin-Yvon model TRIAX320, equipped with a charged coupled device detector (Horiba – SPECTRUM ONE) cooled at -136°C with liquid nitrogen. Twenty scans in the 500-4200 cm^{-1} spectral range were accumulated within a 30s integration time using a 5 cm^{-1} resolution.

The sample was deposited onto a silicon slide, covered by a coverslip glass, and placed on a variable temperature holder (Linkam stage mod. FTIR600 with LNP95 cooling module) to monitor the temperature dependence of the scattered light. Frequency calibration was performed using the spectral lines of silicon. Each sample was cooled down to the lowest temperature at 1 °C/min rate as described for FTIR measurements; Raman spectra were recorded at selected temperature values during heating of the sample at 1 °C/min.

Brillouin Light Spectroscopy

Brillouin light scattering measurements were performed using a single-mode 532 nm solid state laser operated at 75 mW power as excitation source and a 20 cm achromatic lens to focus and collect light from backscattering of the sample. The sample was sandwiched

between an optically polished silicon substrate and a silica glass overlay. Temperature was controlled by the same Linkam stage used for Raman measurements. The scattered light was filtered by a Sandercock-type tandem-multipass Fabry-Perot interferometer [20], recorded and analyzed by a custom made MCA [21]. Inelastically scattered light by thermally activated acoustic modes propagating into the sample is shifted by $\omega = \pm v \cdot q$ with respect to the elastic light, where v is the velocity of the acoustic modes and $q = 2nk_i$ is the momentum exchanged in the back scattering process, n is the refractive index of the sample and k_i the wavevector of the incident light. From this relation, it can be deduced that samples with longitudinal acoustic modes propagating at 2-3 km/s give rise to Brillouin peaks at about 10-20 GHz.

In case of light scattered by damped acoustic modes, a broadening of the Brillouin peaks can also be measured. In this case, the power spectrum of scattered light can be approximated by that of a damped harmonic oscillator (DHO) [22]:

$$I(w) = \frac{I_0}{p} \times \frac{w_b^2 G_b}{(w^2 - w_b^2)^2 + w^2 G_b^2} \qquad (1)$$

where ω_b and Γ_b approximately give the frequency position and linewidth (FWHM) of the Brillouin peaks. These parameters are related to the apparent longitudinal sound velocity, v_L, and viscosity, η_L, through the relations $\omega_b = q\ v_L$ and $\Gamma_b = q^2\ \eta_L/\rho$, where ρ is the mass density. The sound velocity, in turn, is related to the real part of the longitudinal modulus M' through the relationship $M' = \rho v_L^2$. It should be noted that the acoustic modes probed by BLS involve the cooperative motion of molecules with a wavelength of about 200 nm, propagating into the sample through a distance of at least a few wavelengths. BLS is thus sensitive to the collective dynamics of the system rather than to the localized molecular motions detected by IR and Raman spectroscopy.

RESULTS AND DISCUSSION

Figure 1A shows IR spectra of lipids in the 3800-2600 cm^{-1} region. Overall, the IR spectrum of the lipids in water is dominated by the signal from water. Water exhibits a strong vibrational band at around 3300 cm^{-1} arising from OH stretching vibrations. The lipid bands are visible on the shoulder of the water band, and become more pronounced in the dried samples. The symmetric and antisymmetric CH_2 stretching vibrations arising from the lipid acyl chains are visible at 2850 and 2920 cm^{-1}, respectively.

Figure 1B shows the Raman spectra of lipids obtained in the same wavenumber range as the IR spectra. As expected, the intensity of the water signal is reduced with respect to lipid bands compared to that in the IR spectrum. As a consequence, a resolved and complex profile of CH stretching bands is visible in the spectrum of hydrated lipids. In both hydrated and dried lipid samples the two main contributions in the 2700-3050 cm^{-1} spectral region can be assigned to the symmetric and antisymmetric stretching vibrational modes of the methylene groups at around 2850 and 2880 cm^{-1}, respectively. The shoulder at 2928 cm^{-1} can be assigned to a Fermi resonance of the symmetric methyl stretch and the band around 2970 cm^{-1} to the asymmetric methyl stretch of the acyl chains [23,24]. The lipid Raman bands of the sample with trehalose are partially overlapped by the CH stretching bands of the sugar. Fortunately, this overlap is negligible at 2850 cm^{-1}, so this band can be used to study lipid phase behavior.

FTIR and Raman spectra of lipids during heating show shifts of bands in the methylene stretching region associated with the gel to liquid-crystalline phase transition of lipids (Figure 2). Both the symmetric and antisymmetric stretching bands shift to higher wavenumber upon heating. In the Raman spectra, an increase in intensity of the band at 2850

with respect to the band at 2880 cm^{-1} can be observed, which reflects the increase of gauche conformer fraction or the loss of lateral packing of the acyl chains occurring upon melting. Moreover, the main transition is also seen in the 1000-1200 cm^{-1} region of the Raman spectrum (Figure 3). Bands in this region can be assigned to the C-C stretching motions of all-trans (1130 and 1064 cm^{-1}) and gauche (1094 cm^{-1}) segments. A marked increase and red shift of the 1094 cm^{-1} Raman band can be observed with increasing temperature, which likely reflects the rearrangement of acyl chains and the increase in the number of gauche segments coinciding with the melting process. Interestingly, Raman spectra can be used to reveal the coexistence of frozen and non-frozen water below 0 °C (Figure 3B). The OH stretching region of the lipid suspension at T = -25°C shows essentially the same contributions of pure water except for an extra intensity at 3200-3400 cm^{-1}, which likely can be assigned to non-freezable water molecules associated with the hydration layer [25,26].

Figure 4A shows the evolution of Brillouin spectra of a hydrated lipid sample in the temperature range from -30 to 30 °C, showing a large variation in the peak position below 0 °C. It should be noted that the variation at T=0 °C is partially due to the formation of ice. On the other hand, we emphasize that Brillouin peaks of longitudinal acoustic modes from ice are expected at about 19 GHz in the back scattering geometry that was adopted here, [27], which is out of our frequency window. This implies that the Brillouin peaks below 0 °C arise from the propagation of acoustic modes inside lipid domains that remain hydrated, separated from pure ice domains. Below 0 °C some residual water molecules that are not in the ice crystals remain in a liquid-like state, strongly linked to the lipid molecules, as suggested by the Raman spectra of Figure 3B.

The variation of the frequency position of BLS peaks between 0 and -5 °C can partially be attributed to the formation of ice thus inducing a change of the lipid

concentration. Conversely, the variation below -5 °C can be assigned to the characteristic behavior of hydrated lipids below the melting temperature.

The BLS spectra of dried lipids show a smooth temperature evolution of the characteristic frequency of the Brillouin peaks (Figure 4B). Due to the particular scattering geometry that was chosen in the experimental set up, the peaks at about 5GHz are replica of those at about 10 GHz, and they will not be considered in the following.

The BLS spectra of the dried lipid + trehalose sample are quite noisy due to the intense elastic light scattering (Figure 4C). The signal of the acoustic phonons is clearly visible, showing a smooth temperature evolution.

Figure 5 shows the band position of the symmetric CH_2 stretching band, derived from the FTIR and Raman spectroscopy studies, as a function of temperature. The gel to the liquid-crystalline phase transition coincides with a wave number shift from 2851 to 2853 cm^{-1} in the FTIR spectra of hydrated lipids, which is similar to the wavenumber shift observed in the Raman data (from 2851.5 to 2853.5 cm^{-1}). Figure 5 shows that trehalose can prevent the dehydration-induced increase in T_m of PC liposomes. Sugars are known to interact with lipids in the dry state. By interacting with the polar headgroups of phospholipids, sugars depress T_m of model membranes [28,29]. In order to deduce the T_m values from the FTIR and Raman data, the gel to liquid-crystalline phase transition was described as a two state model. Within this model, the band position at temperature T, P_T, can be expressed as [30]:

$$P_T = \frac{P_G + m_G \cdot T + (P_L + m_L \cdot T) K_T}{1 + K_T} \qquad (2)$$

where K_T is the equilibrium constant at temperature T between the two states, P_G and P_L are the values of P_T at T=0 K in the gel and liquid state respectively, and m_G and m_L give their temperature dependence, which is approximated as linear behavior in the analyzed region. The equilibrium constant K_T can be expressed as a function of the melting temperature T_m according to equation:

$$\ln(K_T) = C\left(\frac{1}{T_m} - \frac{1}{T}\right) \quad (3)$$

where C is proportional to the melting enthalpy. A non-linear least squares method has been used to fit the experimental data in Fig. 5 with equations 2 and 3 and the obtained T_m values are reported in Table 1.

FTIR measurements indicate that hydrated liposomes have a T_m at approximately -7 °C. The T_m increases to 34 °C when liposomes are dried in the absence of trehalose, whereas in the presence of trehalose the *Tm* decreases to -21 °C, far below that of the hydrated control. Thus, the lipid bilayer remains in the liquid crystalline phase during dehydration at room temperature (22 °C). The T_m values derived from the Raman spectra closely resemble those of the FTIR spectra: T_m values were found to be -6, 29 and -27 °C for hydrated lipids, dried lipids, and lipids dried with trehalose. The slight differences in T_m values of the dried samples compared to those obtained from the FTIR spectra are likely due to small differences in water content. Small differences in water content have a great effect on T_m of dried lipids.

Figure 6A shows the frequency shift and Figure 6D the linewidth of BLS spectra of the hydrated lipid sample. The frequency shift displays a similar behavior compared to that of aligned multilamellar samples studied by BLS [31]. In the latter case the cusp-like temperature behavior of the longitudinal elastic modulus was assigned to the liquid-crystalline to gel phase transition of lipids. It should be noted that in the present study, the elastic properties averaged over different directions with respect to the acyl chains in a heterogeneous non-aligned multilamellar sample have been probed. This implies that despite the disordered nature of the samples the melting transition of the lipids can still be observed. On the other hand, the jump in the value of the frequency shift occurring between 0 and -5 °C can partially be attributed to the change in lipid concentration induced by ice formation. The linewidth (lower panel) stays almost constant in the ordered phase and decreases with increasing temperature in the disordered phase. This behavior is dominated by the water

viscosity as confirmed by the data of pure water deduced from previous BLS and ultrasonic experiments [32,33] and reported for sake of comparison as a line in Fig. 6D.

Figure 6B shows the frequency shift and Figure 6E the linewidth of the BLS spectra of dried lipids. The transition temperature corresponds to a smooth change in the temperature dependence of the Brillouin frequency shift. The effect of the transition on the collective properties (propagation of acoustic modes) is much less pronounced compared to that observed in the hydrated lipids. In fact, the acoustic properties of the dried lipids are typical of a viscoelastic fluid, affected by relaxation processes. The presence of a strong relaxation active in the GHz frequency range is evident from the pronounced maximum in the acoustic absorption, i.e. in the Brillouin linewidth, at about 45 °C. The characteristic time of this relaxation process is given by $\tau = 1/\omega_b \approx 14$ ps at 45 °C. A dispersion in the velocity of the acoustic modes associated with this absorption must be taken into account, i.e. a bending in the temperature dependence of Brillouin frequency, which can partially mask the effect of the melting transition of the lipid. Concerning the microscopic origin of this relaxation process, it is interesting to note that a relaxation with similar characteristic times revealed by BLS in polybutadiene has been attributed to conformational changes induced by thermally activated rotations around $–CH_2\text{-}CH=$ bonds of the polymeric backbone [34,35]. In the same time range a hypersonic relaxation process has been also observed in a simple liquid alkanol, suggesting a coupling between hydrodynamic modes and the local molecular change of acyl chain structure [36]. Similar conformational fluctuations are also present in lipid acyl chains and the coupling of the associated density fluctuations with acoustic modes may be responsible for the observed relaxation process.

Figure 6C shows the frequency shift and Figure 6F the linewidth of BLS spectra of the dried lipid + trehalose sample. The signature of the melting transition in the temperature dependence of the Brillouin frequency shift is more clearly visible compared to that of lipids

dried in the absence of trehalose. In this case no clear signatures of relaxation processes are observed in the investigated temperature range, so that the change in the slope of ω_b can be entirely assigned to the melting transition. The absence of strong relaxations and the higher value of the sound velocity are both connected to the amorphous behavior of the sample. In fact, the good glass-forming properties of trehalose are connected to its protective actions during drying. Moreover, some water molecules are usually trapped between sugar and lipid molecules. The very large value of the Brillouin linewidths may be due to the presence of micrometric heterogeneities in the sample, which are also responsible for both the scattering of phonons and the intense elastic scattering of photons giving rise to the huge elastic contribution in the spectra.

CONCLUSIONS

Fourier transform infrared, Raman and Brillouin spectroscopy are complementary techniques that can be used to study different aspects of lipid phase behavior of hydrated as well as dried lipid systems. In particular, the methylene C-H stretching region in IR and Raman spectra can be used to study the rearrangement of lipid acyl chains occurring at the lipid melting temperature. IR spectra have a higher signal to noise ratio, thus permitting a more precise evaluation of the melting temperature. In the hydrated lipid samples, the CH stretching region in the Raman spectra is less affected by the contribution of water compared to that in the IR spectra. Raman spectra are particularly suitable to simultaneously study both lipid and water contributions allowing to distinguish ice from non-frozen water below the freezing point of water.

The gel to liquid-crystalline phase transition coincides with an increase in wave number position of the symmetric CH_2 stretching band in both FTIR and Raman spectra. Raman and

FTIR yield similar Tm values for hydrated as well as dried lipids. The phase transition temperature, Tm, increases when liposomes are dried. When liposomes are dried in the presence of trehalose, however, the Tm decreases compared to that of the hydrated control. By interacting with the polar headgroups of phospholipids, trehalose can prevent the dehydration-induced increase in Tm of PC liposomes.

The collective dynamics measured by BLS is rich of information on phase changes and on the molecular rearrangement occurring in lipid membranes. Sound velocity in the hydrated sample shows visible changes due to the partial freezing of water and to gel – liquid crystal transition already observed in oriented lipid membranes. In the same sample the acoustic attenuation in the disordered phase is dominated by viscosity of water. The dried sample with trehalose shows solid-like properties, with a change to a more anharmonic behavior when increasing temperature across the phase transition. In this case, the linewidth of Brillouin lines is dominated by the heterogeneous nature of the sample rather than by acoustic damping.

The relaxation of density fluctuations revealed by BLS in the disordered phase of the dried sample without trehalose suggests the existence of a dynamic disorder, with conformational changes occurring in the tens of picosecond time scale. The melting transition probed by vibrational spectroscopies allows to better interpret this process supporting the rearrangement of lipid chains in the liquid phase to be the molecular origin of this relaxation. Series of measurements performed at different exchanged wave-vectors could help to obtain the activation energy of this process and, together with molecular dynamics simulations, to confirm its molecular origin.

Acknowledgements: Authors acknowledge the Centro Nazionale Trapianti for financial support by the project “Crioconservazione di cellule per uso clinico umano, con particolare riferimento ad alcune tipologie come le cellule staminali emopoietiche, mesenchimali e cellule riproduttive”. S.C. acknowledges support from MIUR-PRIN (Project 2012J8X57P) and PAT (Autonomous Province of Trento) “Grandi Progetti 2012” Project “MaDEleNA” W.W. acknowledges support from the German Research Foundation (Deutsche Forschungsgemeinschaft, DFG) via the Cluster of Excellence ‘From regenerative biology to reconstructive therapy’ (REBIRTH) and grant WO-1735/6-1. H.O. acknowledges support from the DFG via grant SI-1462/4-1.

REFERENCES

[1] M. Caffrey, J. Hogan, *Chem. Phys. Lipids* **1992**, *61*, 1.

[2] H.H. Mantsch, R.N. McElhaney, *Chem. Phys. Lipids* **1991**, *57*, 213.

[3] M. Caffrey, *Biochim. Biophys. Acta* **1987**, *896*, 123.

[4] L.M. Crowe, J.H. Crowe, D. Chapman, *Arch. Biochem. Biophys.* **1985**, *236*, 289.

[5] W.F. Wolkers, H. Oldenhof, B. Glasmacher, *Cryobiology* **2010**, *61*, 108.

[6] R.N. Lewis, R.N. McElhaney, *Methods Mol. Biol.*, **2007**, *400*, 207.

[7] A.V. Popova, D.K. Hincha, *BMC Biophysics* **2013**, *6*, 9.

[8] W.F. Wolkers, in *Biological and Biomedical Infrared Spectroscopy*, (Eds: A. Barth, P.I. Haris), IOP Press, Amsterdam, **2009**, 272.

[9] G. Cazzolli S. Caponi, A. Defant, C. M. C. Gambi, S. Marchetti, M. Mattarelli, M. Montagna, B. Rossi, F. Rossi and G. Viliani, *J. Raman Spectrosc.*, **2012**, *43*, 1877.

[10] S. Caponi, L. Liguori, A Giugliarelli, Mattarelli, M., Morresi, A., Sassi, P., Urbanelli, L., Musio, C , *Biophys. Chem.* **2013,** *182*, 58.

[11] B.P. Gaber, W.L. Peticolas, W.L., *Biochim. Biophys. Acta* **1977**, *465* 260.

[12] N. Yellin, I.W. Levin, *Biochim. Biophys. Acta* **1977**, *489*, 177.

[13] C.B. Fox, R.H. Uibel, J.M. Harris, *J. Phys. Chem. B* **2007**, *111*, 11428.

[14] F. Scarponi, L. Comez, D. Fioretto, and L. Palmieri, *Phys. Rev. B*, **2004**, *70*, 054203.

[15] S. Caponi, S Corezzi, M Mattarelli, D Fioretto, *J. chem. phys.*, **2014**, *141*, 214901.

[16] F. Palombo, C. P. Winlove, R. S. Edginton, E. Green, N. Stone, S. Caponi, M. Madami, D. Fioretto, *J. R. Soc. Interface*, **2014**, *11*, 20140739.

[17] M.Y. El-Sayed, T.A. Guion, and M.D. Fayer, *Biochemistry*, **1986**, *25*, 4825.

[18] J.P. LePesant, L. Powers, P. S. Pershan, *Proc. Natl. Acad. Sci. U.S.A.*, **1978**, *75*, 1792.

[19] M.C. Rheinstädter, C. Ollinger, G. Fragneto, F. Demmel,and T. Salditt, *Phys. Rev. Lett.* **2004**, *93*, 10810.

[20] F. Nizzoli, J.R. Sandercock, in: G.K. Horton, in *Dynamic Properties of Solids* (Eds: A.A. Maradudin), Amsterdam, North-Holland, vol. 6, **1990**, 307.

[21] D. Fioretto. F. Scarponi, *Mat. Sci. Eng. A-Struct*, **2009,** *A 521–522*, 243

[22] D. Fioretto, L. Comez, G. Socino, L. Verdini, S. Corezzi, P.A. Rolla, *Phys. Rev. E*, **1999**, *59*, 1899.

[23] K. G. Brown, *J. Phys. Chem.*, **1987**, *91*, 3436.

[24] M.J.L. de Lange, M. Bonn, M. Müller, *Chem. Phys. Lipids*, **2007**, *146*, 76.

[25] H. Abramczyk,, B. Brozek-Pluska, M. Krzesniak, M. Kopec, A. Morawiec-Sztandera, *Spectrochim. Acta Part A*, **2014**, *129*, 609.

[26] M.E. Gallina, P. Sassi, M. Paolantoni, A. Morresi, R.S. Cataliotti, *J. Phys. Chem. B*, **2006**, *110*, 8856.

[27] P.H. Gammon, H. Klefte,' and M. J. Clouter, *J. Phys. Chem,.*, **1983**, *87*, 4025

[28] J.H. Crowe, , F. A. Hoekstra, K. H. N. Nguyen, L. M. Crowe, *Biochim. Biophys. Acta*, **1996**, *1280*, 187.

[29] J.H. Crowe, F.A. Hoekstra, L.M. Crowe, *Annu. Rev. Physiol.*, **1992**, *54*, 579.

[30] P.Sassi, A. Giugliarelli, M. Paolantoni, A. Morresi, G. Onori, *Biophys. Chem.*, **2011**, *158*, 46.

[31] J.-P. Lepesant, L. Powers, P. S. Pershan, *Proc. Nati. Acad. Sd.*, **1978**, *75*, 1792

[32] A. Cunsolo, M. Nardone, *J.Chem.Phys*., **1996**, *105*, 3911.

[33] S.Hawley, J.Allegra, G.Holton, *J. Acous. Soc. Am.*, **1970**, *47*, 137.

[34] D.Fioretto, M.Mattarelli, C.Masciovecchio, G.Monaco, G.Ruocco, F.Sette, *Phys. Rev. B*, **2002**, *65*, 224205.

[35] A. Aoudi, M.J. Lebon, C. Dreyfus, B. Strube, W. Steffen, A. Patkowski, and R.M. Pick, *J. Phys.: Condens. Matter*, **1997**, *9*, 3803.

[36] P. Sassi, M. Paolantoni, A. Morresi, *Chem. Phys. Lett.*, **2002**, *357*, 293.

Table 1. T_m values deduced from FTIR and Raman data according to fit with Eqs. (2) and (3)

Technique\ T_m(°C)	Dried	hydrated	dried+trehalose
IR	33.9±2.0	-6.5±0.4	-21.4±1.2
Raman	29.4±2.5	-6.2±1.6	-26.6±2.0

FIGURE LEGENDS

Figure 1. IR (1A) and Raman (1B) spectra of hydrated and dried multilamellar L-α-phosphatidylcholine assemblies in the 3800-2600 cm^{-1} region.

Figure 2. IR (2A, 2B and 2C) and Raman (2D, 2E and 2F) spectra of the CH stretching region of hydrated EPC (2A and 2D), dried EPC (2B and 2E) and dried EPC+trehalose (EPC/trehalose: 1/2 weight ratio; 2C and 2F). The appropriate temperature ranges are selected in order to follow the melting transition of EPC in each sample.

Figure 3. Raman spectra of hydrated PC lipids. Panel A: skeletal vibrations of EPC in hydrated sample.Panel B: Raman spectra of the OH stretching region of pure H_2O (dashed line) and of the hydrated lipid suspension (solid line) at T = -25°C.

Figure 4. Brillouin spectra of hydrated EPC (4A), dried EPC (4B) and dried EPC+trehalose (4C) at different temperatures. BLS spectra show the characteristic Brillouin doublets in the GHz frequency range, due to the scattering of light from longitudinal acoustic modes propagating into the sample.

Figure 5. Wavenumber position of the CH_2 symmetric stretching band of lipid acyl chains obtained from IR (5A) and Raman (5B) spectra. A sigmoidal temperature behavior delimits the melting transition. The continuous line is obtained by fitting the data with Eqs. 2 and 3.

Figure 6. Brillouin frequency shift ($\omega_b/2\pi$) and linewidth ($\Gamma/2\pi$) of hydrated EPC (6A and 6D), dried EPC (6B and 6E) and dried EPC+trehalose (6C and 6F) as a function of

temperature, obtained by a fitting procedure of BLS spectra with the DHO function of Eq.1, convoluted with the instrumental resolution function. In figure 6B full line is referred to pure water attenuation data.

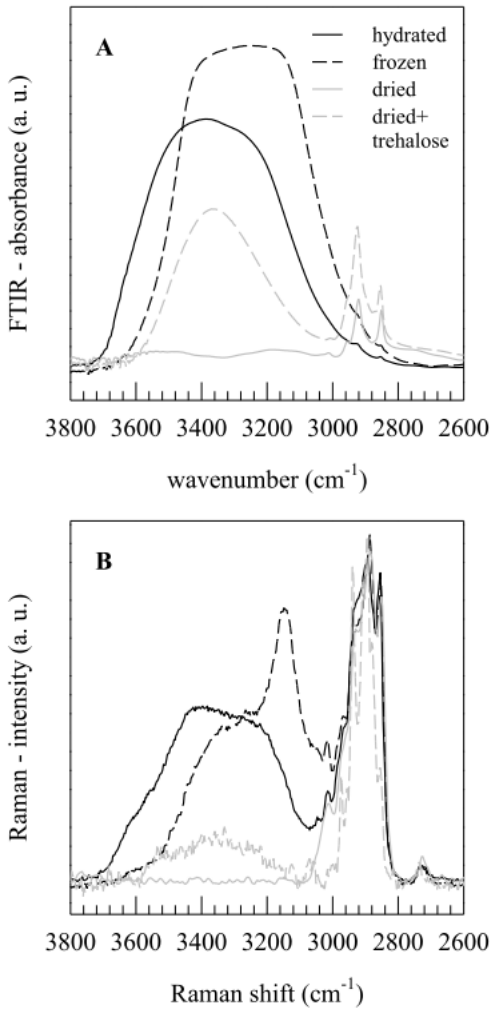

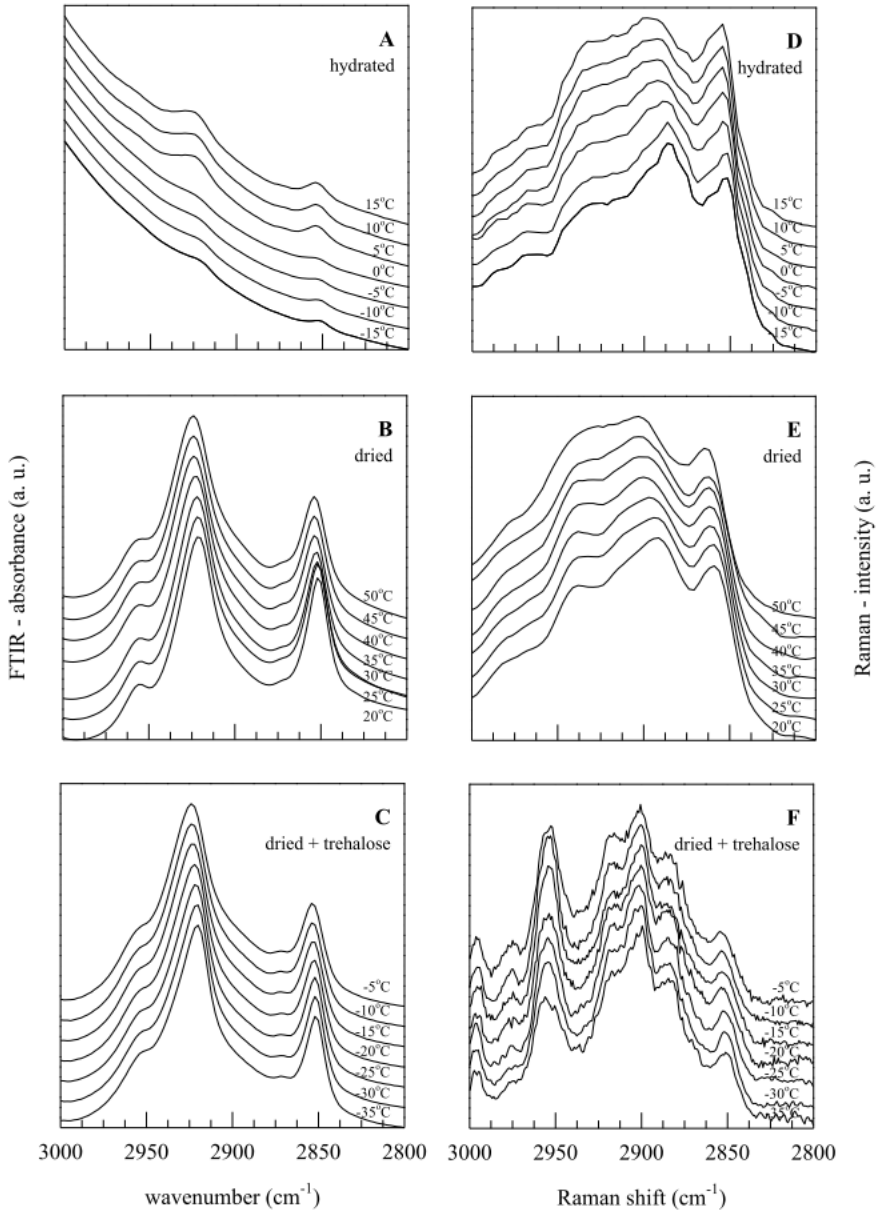
A
hydrated
15°C
10°C
5°C
0°C
-5°C
-10°C
-15°C
D
hydrated
15°C
10°C
5°C
0°C
-5°C
-10°C
-15°C
B
dried
50°C
45°C
40°C
35°C
30°C
25°C
20°C
E
dried
50°C
45°C
40°C
35°C
30°C
25°C
20°C
C
dried + trehalose
-5°C
-10°C
-15°C
-20°C
-25°C
-30°C
-35°C
F
dried + trehalose
-5°C
-10°C
-15°C
-20°C
-25°C
-30°C
-35°C
FTIR - absorbance (a. u.)
Raman - intensity (a. u.)
3000
2950
2900
2850
2800
wavenumber (cm-1)
Raman shift (cm-1)

1

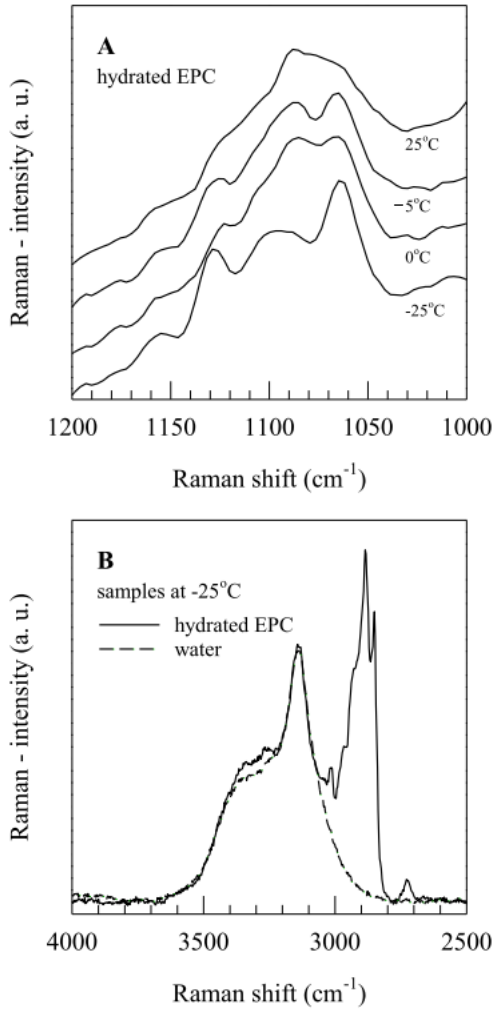
A
hydrated EPC
25°C
−5°C
0°C
-25°C
Raman - intensity (a. u.)
1200
1150
1100
1050
1000
Raman shift (cm-1)
B
samples at -25°C
hydrated EPC
water
Raman - intensity (a. u.)
4000
3500
3000
2500
Raman shift (cm-1)

1

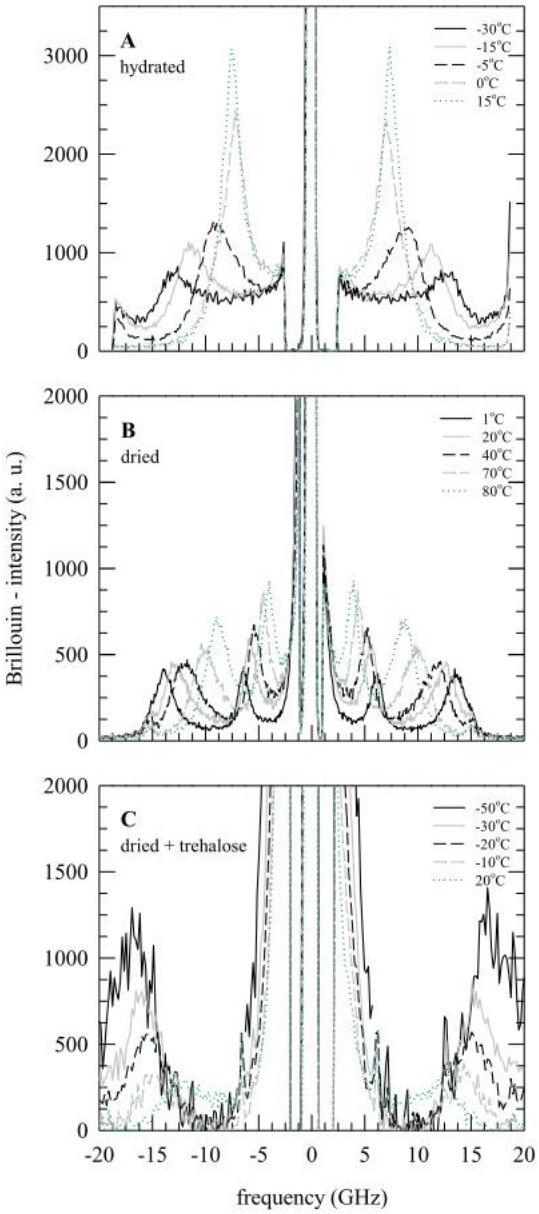
A
hydrated
-30°C
-15°C
-5°C
0°C
15°C
B
dried
1°C
20°C
40°C
70°C
80°C
C
dried + trehalose
-50°C
-30°C
-20°C
-10°C
20°C
Brillouin - intensity (a. u.)
frequency (GHz)

1

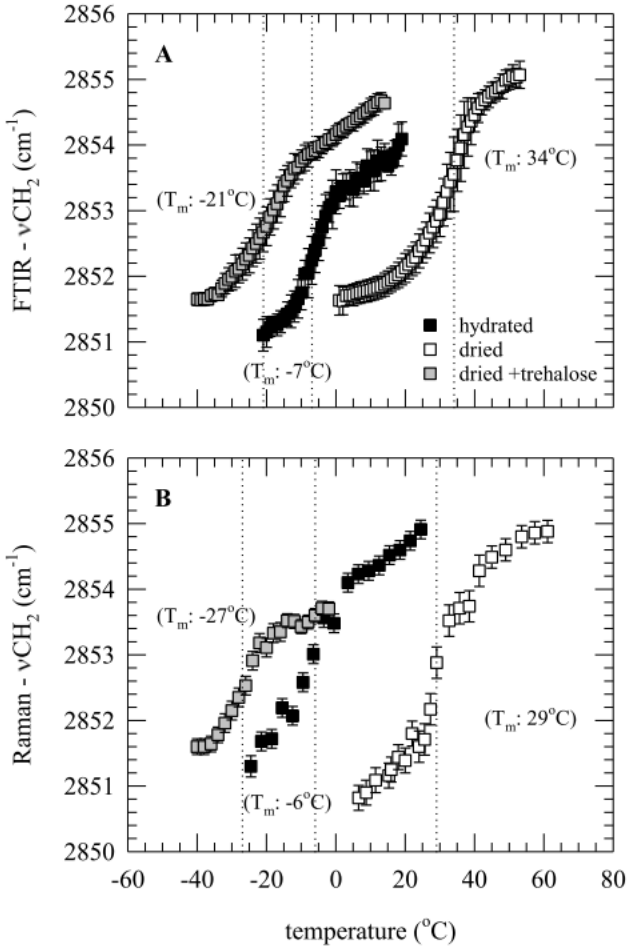
A
B
FTIR - νCH2 (cm-1)
Raman - νCH2 (cm-1)
(Tm: -21°C)
(Tm: -7°C)
(Tm: 34°C)
hydrated
dried
dried +trehalose
(Tm: -27°C)
(Tm: -6°C)
(Tm: 29°C)
temperature (°C)
2856
2855
2854
2853
2852
2851
2850
-60
-40
-20
0
20
40
60
80

1

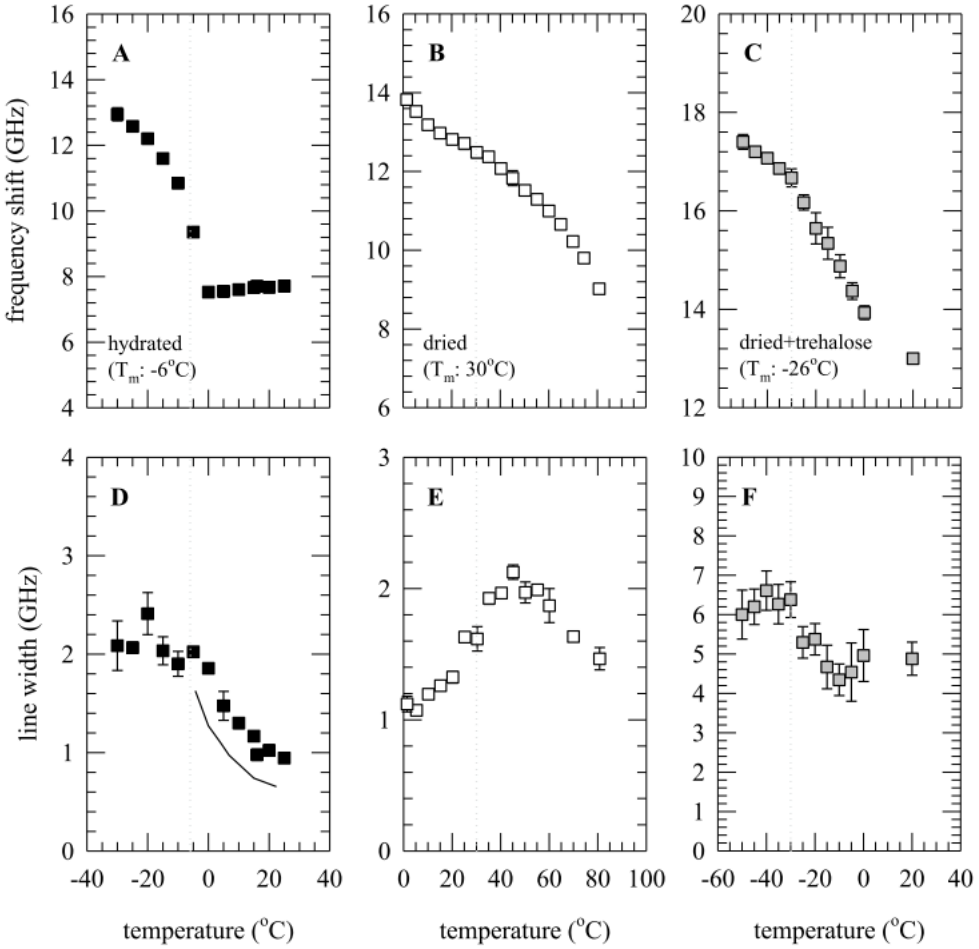
A
B
C
D
E
F
frequency shift (GHz)
line width (GHz)
hydrated
(T_m: -6°C)
dried
(T_m: 30°C)
dried+trehalose
(T_m: -26°C)
temperature (°C)
temperature (°C)
temperature (°C)

1